# Excitation of non-normal parity states by pion scattering: Application to $^{13}C$

T.-S. H. Lee and D. Kurath
*Argonne National Laboratory, Argonne, Illinois 60439*
(Received 17 April 1980)

General features are calculated for excitation of non-normal parity states in pion scattering on $1p$-shell targets. Detailed distorted-wave impulse approximation results are given for $^{13}C$ and related to effects of nuclear structure. Approximate formulas are deduced and applied to the region of excitation energy from 10 to 23 MeV. Calculations for $(e,e')$ in this region are included.

[NUCLEAR REACTIONS, NUCLEAR STRUCTURE $(\pi,\pi')$ $E_\pi \approx 160$ MeV; $d\sigma/d\Omega$ for $^{13}C$ based on DWIA in momentum space; comparison of calculated $(e,e')$ and $(\pi,\pi')$; effects of nuclear structure.]

## I. INTRODUCTION

In a recent paper[1] we presented the formalism for the treatment of inelastic scattering of pions with energy near the (3,3) resonance with the distorted wave impulse approximation (DWIA) in momentum space. Calculated results were presented for excitation of states of normal parity, $(1p)^n$, in all $1p$-shell targets. In this paper we extend the treatment to excitation of states of non-normal parity, $(2sd)^1(1p)^{n-1}$, in $(1p)^n$ targets. In Sec. II we discuss general features resulting from the calculation of such parity-changing particle-hole excitations. Section III contains the detailed results for $^{13}C$ together with estimates of excitation of such states by inelastic electron scattering. Section IV contains the discussion and summary.

## II. GENERAL FEATURES

The kind of excited state under discussion is reached by acting on the $(1p)^n(0s)^4$ target state with particle-hole operators $(2sd)^1(1p)^{-1}$ or $(1p)^1(0s)^{-1}$. As in Ref. 1 our results are more clearly interpreted in terms of the $LS$ representation of these operators. The nuclear structure input to the DWIA calculation is obtained by specializing Eq. (19) of Ref. 1.

$$F_{LS}^{fiJT}(r) = \sum_l \langle J_f T_f \| [b_{2l}^\dagger \times h_{1p}^\dagger]_{J(LS)T} \| J_i T_i \rangle \times (6\hat{J}\hat{l})^{1/2} \begin{pmatrix} l & 1 & L \\ 0 & 0 & 0 \end{pmatrix} R_{2l}(r) R_{1p}(r) , \quad (1)$$

wherein $l=0$ or 2 and the nuclear matrix element is evaluated for $T_3 = T_i$. We omit the $(1p)^1(0s)^{-1}$ excitation which plays a minor role in our results. From Eq. (1) we see that since $l$ is even the only $L$ values which contribute to our DWIA calculation are $L=1$ and $L=3$.

Each of the $J(LS)$ terms leads to a distinctive angular distribution, and Figs 1–5 show the cross sections resulting from individual amplitudes calculated for $\pi^+$ beams at 162 MeV on $^{13}C$. The $J(LS)$ structure amplitudes have been normalized to unity in obtaining these figures and separate calculations are shown for $l=0$ and $l=2$. Of course in calculating cross sections for exciting a particular nuclear state, all terms with the same $J$ contribute coherently with weights given by the particle-hole amplitudes for that state, but often a single term is dominant. From the figures one sees that only a few amplitudes will lead to strong transitions, and that these have distinctive features.

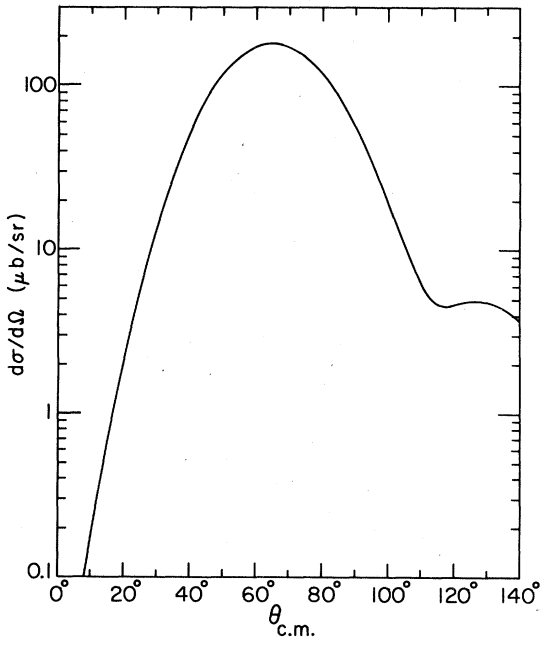


FIG. 1. Differential cross section for excitation of $^{13}C$ by 162 MeV pions for $J(LS)=4(31)$.

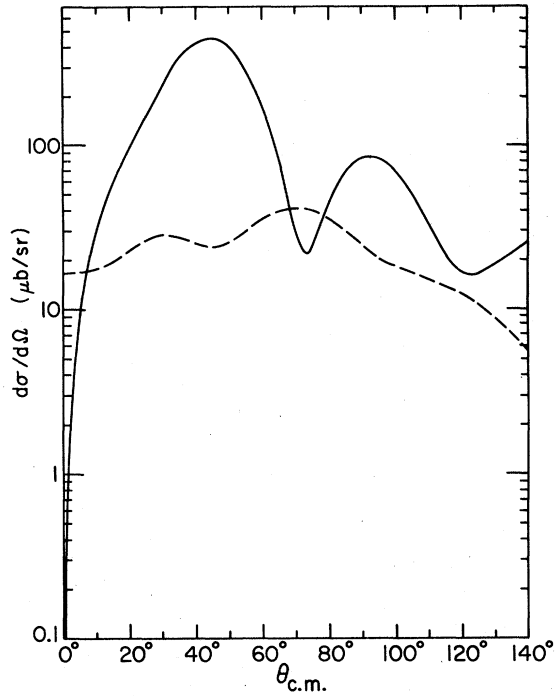


FIG. 2. Differential cross section for excitation of $^{13}C$ by 162 MeV pions for $J(LS)=3(30)$ (solid line) and 3(31) (broken line).

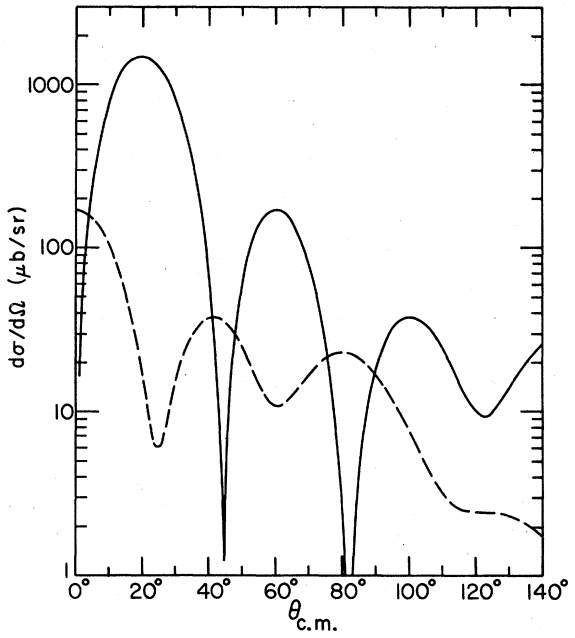


FIG. 4. Differential cross section for excitation of $^{13}C$ by 162 MeV pions via $2sp^{-1}$ for $J(LS)=1(10)$ (solid line) or 1(11) (broken line).

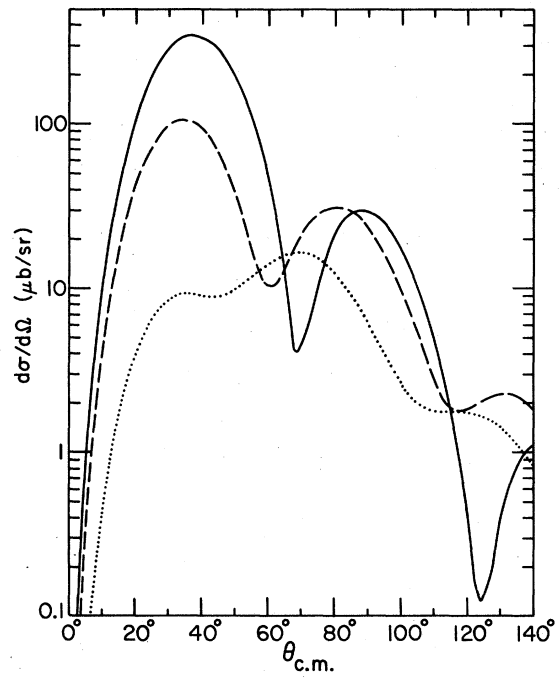


FIG. 3. Differential cross section for excitation of $^{13}C$ by 162 MeV pions for $J(LS)=2(11)$ via $dp^{-1}$ (solid line) or $2sp^{-1}$ (broken line) or via 2(31) (dotted line).

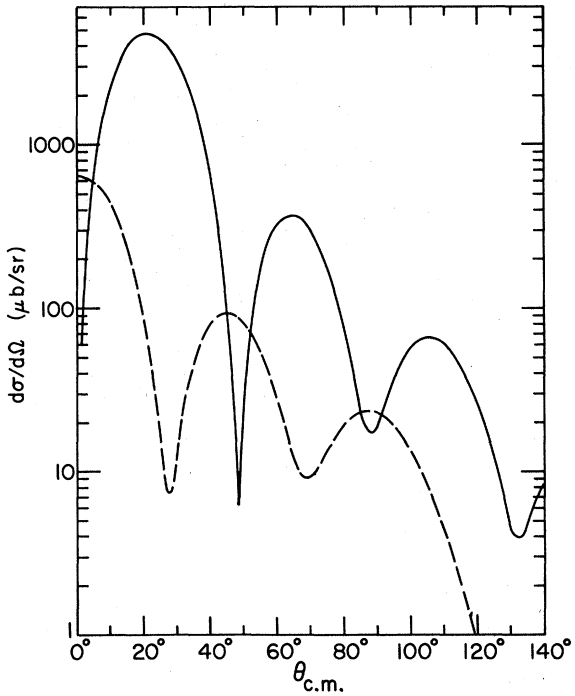


FIG. 5. Differential cross section for excitation of $^{13}C$ by 162 MeV pions via $dp^{-1}$ for $J(LS)=1(10)$ (solid line) or 1(11) (broken line).

For $J=4$ there is only one amplitude $(LS)=(31)$, and the cross section in Fig. 1 has a broad peak around 65°. The $J=3$ cross sections of Fig. 2 show the dominance of the (30) term, which has a first maximum at 45°. In Fig. 3 one sees that for $J=2$ the (11) amplitudes lead to much larger cross sections than the (31) amplitude, and that the $dp^{-1}$ amplitude contributes more strongly than the $2sp^{-1}$ amplitude with both giving first maxima about 35°. Finally, Figs. 4 and 5 show that for $J=1$ the (10) amplitudes give large cross sections, again $dp^{-1}$ contributes more strongly and that first maxima occur around 20°. The $p0s^{-1}$ cross sections are very similar to the $2sp^{-1}$ cases of Fig. 4 but the weights of such terms are generally small in states below 25 MeV excitation. The $J=0$ amplitude does not contribute in our DWIA calculation as can be seen in Eq. (10) of Ref. 1. From the figures one sees that strong transitions arise from the amplitudes with $J(LS)$ equal to 4(31), 3(30), 2(11), and 1(10) which lead to distinctive shapes with first maxima at smaller angles with smaller $J$.

These features are very useful in identifying strong transitions, particularly for a $J=0$ target such as $^{12}$C, since only a single $J$ contributes to each transition. For targets of higher $J$ the angular distributions would be much flatter if several $J$ values contribute. The greatest benefit of these results is that one can make approximate formulas to estimate the cross sections for any state given the matrix elements of the one body transition density resulting from a nuclear structure calculation. The more lengthy DWIA calculations need only be done for cases of special interest. This approach is used in our survey of excitations in $^{13}$C.

## III. APPLICATION TO $^{13}$C

### A. The nuclear model

The non-normal parity states for $^{13}$C are obtained from a shell model calculation within the $1\hbar\omega$ space $(0s)^3(1p)^{10}$ plus $(0s)^4(1p)^8(2sd)^1$, removing states of spurious center-of-mass excitation. This is a slight modification of an earlier calculation by Millener and Kurath,[2] with the same two-body interactions but increased single-particle energies of the $2sd$ levels in order to raise the energies of the positive-parity levels relative to the ground state. The numerical values for the $s_{1/2}$, $d_{5/2}$, and $d_{3/2}$ levels were changed from 5.34 to 5.52, 10.43 to 11.15, and 11.86 to 12.95 MeV, respectively. The resulting spectrum of positive-parity states is given in Fig. 6 together with experimentally identified states up to 10 MeV in $^{13}$C. There is a close correspondence between calculation and experiment for the lower spectrum. Above 12 MeV the density of states increases rapidly even within the restricted $1\hbar\omega$ space. Nevertheless, one can get some idea of the location of strength for inelastic pion scattering and electron scattering.

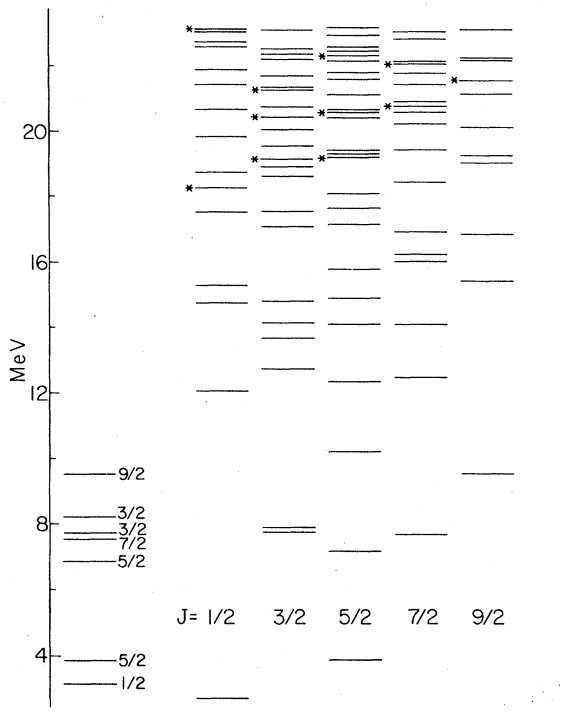


FIG. 6. Energy level spectrum for $^{13}$C with experiment on the left and calculated levels separated according to $J$. Levels with $T=\frac{3}{2}$ are denoted by an asterisk.

### B. The low-lying states

In Figs. 7–12 we give the calculated cross sections for excitation of the seven positive-parity

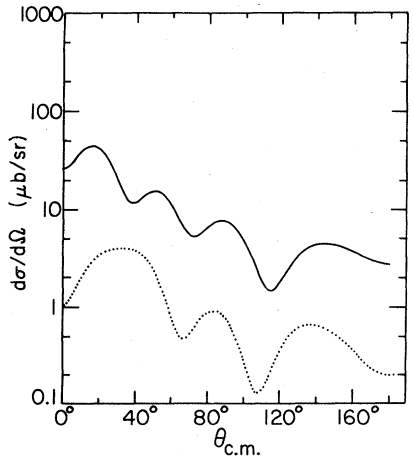


FIG. 7. Cross sections calculated for excitation of the $J_f=\frac{1}{2}^+$ state at 3.09 MeV in $^{13}$C by 162 MeV $\pi^-$ (solid line) or $\pi^+$ (dotted line) beams.

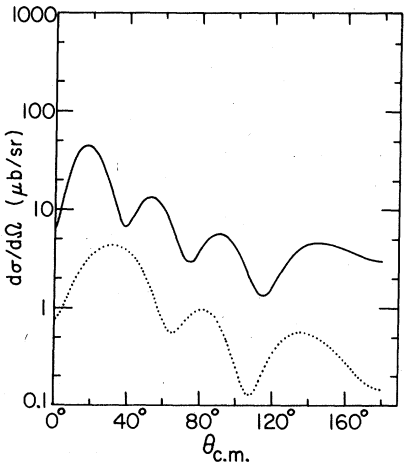


FIG. 8. Cross sections calculated for excitation of the $J_f = \frac{3}{2}^+$ state at 7.68 MeV in $^{13}C$ by 162 MeV $\pi^-$ (solid line) or $\pi^+$ (dotted line) beams.

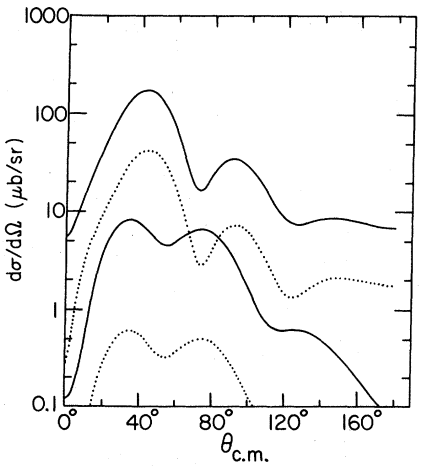


FIG. 10. Cross sections calculated for excitation of the $J_f = \frac{5}{2}^+$ state at 3.85 MeV (upper curves) and 6.86 MeV (lower curves) in $^{13}C$ by 162 MeV $\pi^-$ (solid line) or $\pi^+$ (dotted line) beams.

states below 10 MeV by inelastic $\pi^\pm$ scattering at 162 MeV. A feature common to all these states is that the cross section for $\pi^-$ scattering is calculated to be considerably larger than that for $\pi^+$ scattering. This is understandable in terms of the nuclear structure of the states since the low lying positive parity states are quite well represented by a weak-coupling picture in terms consisting of a $2sd$ neutron coupled to low $T=0$ states of $^{12}C$. The transitions from the ground state are thus mainly neutron transitions, which favors $\pi^-$ scattering.

The calculated excitation of the $\frac{1}{2}^+$ state near 3 MeV is shown in Fig. 7. The $\pi^-$ curve shows a first maximum near 20°, as do the $(LS)=(10)$ curves, but the effects of the (11) amplitudes are clearly present. The $\pi^+$ cross section is very weak and the shape means the (10) and (11) amplitudes are of similar magnitude. In these low-lying states, the (10) strength is generally inhibited with the $dp^{-1}$ and $2sp^{-1}$ contributions interfering destructively. If we used only the $2sp^{-1}$ transition density matrix elements in the calculation, the peak cross sections would be 320 $\mu$b for $\pi^-$ excitation compared to 44 $\mu$b in Fig. 7, and 60 $\mu$b for $\pi^+$ excitation. A similar cancellation is known from calculating $E1$ gamma transitions for low-lying states and it clearly carries over to pion scattering.

The transitions to the two $\frac{3}{2}^+$ states, experimentally at 7.7 and 8.2 MeV, are also calculated

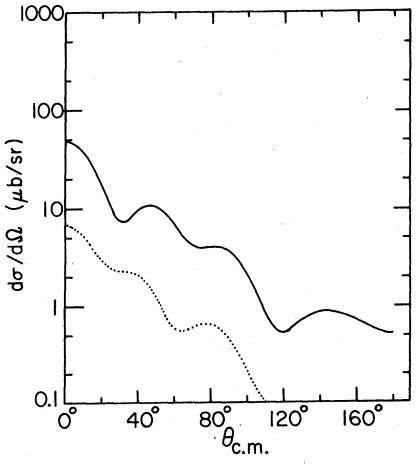


FIG. 9. Cross sections calculated for excitation of the $J_f = \frac{3}{2}^+$ state at 8.2 MeV in $^{13}C$ by 162 MeV $\pi^-$ (solid line) or $\pi^+$ (dotted line) beams.

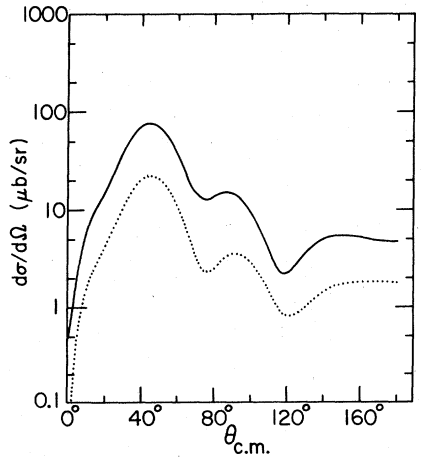


FIG. 11. Cross sections calculated for excitation of the $J_f = \frac{7}{2}^+$ state at 7.49 MeV in $^{13}C$ by 162 MeV $\pi^-$ (solid line) or $\pi^+$ (dotted line) beams.

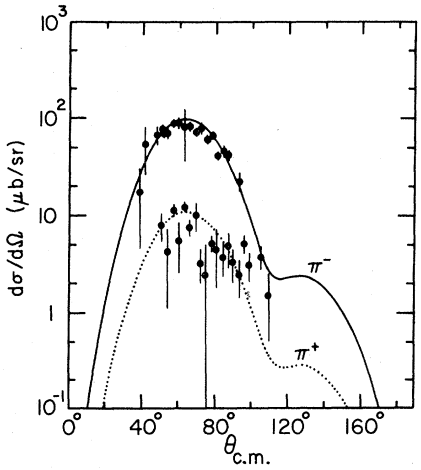


FIG. 12. Cross sections calculated for excitation of the $J_f = \frac{9}{2}^+$ state at 9.50 MeV in $^{13}$C by 162 MeV $\pi^-$ (solid line) or $\pi^+$ (dotted line) beams. Data points were supplied by Ref. 4.

to be very weak, as seen in Figs. 8 and 9, except for $\pi^-$ scattering to the lower state which has a (10) shape and a peak magnitude of 45 $\mu$b, about the same as calculated for the $\frac{1}{2}^+$ state. Also the shapes are sensitive since these states are nearly degenerate in calculated energy, so that small changes in the calculation input can mix them strongly. The most reliable quantity is the summed cross section for excitation of both states.

The transitions to the two $\frac{5}{2}^+$ states, experimentally at 3.85 and 6.85 MeV, are shown in Fig. 10. While both $J=2$ and 3 can contribute here, the transitions to the lower state clearly have the $(LS)=(30)$ shape of Fig. 2, with peak cross sections of 170 $\mu$b for $\pi^-$ scattering and 40 $\mu$b for $\pi^+$ scattering. Transitions to the upper state are calculated to be very weak and dominated by $J=2$ contributions. The transition to the $\frac{7}{2}^+$ state, experimentally at 7.5 MeV, is calculated to have the (30) shape with peak cross sections of 75 $\mu$b for $\pi^-$ scattering and 22 $\mu$b for $\pi^+$ scattering as shown in Fig. 11.

The $\frac{9}{2}^+$ state at 9.5 MeV is a pure $J=4$ transition so it must have the (31) shape of Fig. 1. The calculated result is shown in Fig. 12 and gives peak cross sections of 97 $\mu$b for $\pi^-$ scattering and 11 $\mu$b for $\pi^+$ scattering. The experimental assignment of $J=\frac{9}{2}^+$ for the 9.5-MeV state comes from recent results[3] of inelastic pion scattering. We have included the data from these experiments[4] in Fig. 12, and the agreement is very good considering that the weak $\pi^+$ points are difficult to measure.

There are experimental difficulties in obtaining data for comparison with the calculations of excitation of these low-lying positive-parity states. The $\frac{1}{2}^+$ and $\frac{3}{2}^+$ states are weak and of reasonable strength only at the forward angles with peaks around 15° to 20°. The fairly strong transition to the lower $\frac{5}{2}^+$ state is masked by excitation of a stronger $\frac{3}{2}^-$ state nearby which has peak cross sections of about 1 mb in both $\pi^\pm$ scattering. A similar situation exists for the $\frac{7}{2}^+$ state since there is a stronger $\frac{5}{2}^-$ state only 60 keV away. Only the $\pi^-$ excitation of the $\frac{9}{2}^+$ state is easy to measure. There are two current measurements of inelastic pion scattering[3,5] on $^{13}$C which indicate reasonable agreement with our calculation for the $\frac{9}{2}^+$ state and earlier calculations[1] of the strong $\frac{3}{2}^-$ and $\frac{5}{2}^-$ states.

### C. Approximate cross section formulas

Since only a few $J(LS)$ values contribute to strong transitions it is useful to have approximate formulas for estimating cross sections given the nuclear structure input. The formulas are expressed in terms of transition density matrix elements for neutrons and protons as in Eq. (21) of Ref. 1, specialized for $(2sd)^1(1p)^{-1}$ transitions in $^{13}$C:

$$A_{J(LS)lt_3} \equiv \langle J_f T_f \| [b^{2l\dagger}_{t_3} \times \tilde{b}^{1p}_{t_3}]_{J(LS)} \| \tfrac{1}{2}^- \tfrac{1}{2} GS \rangle , \qquad (2)$$

where $t_3$ is neutron or proton and $\tilde{b}$ is the $1p$ hole-creation operator. The general estimated cross sections at first forward maxima are given by

$$\frac{d\sigma}{d\Omega}(\pi^+, \theta_{\text{peak}}, J) \simeq C_J (J_f + \tfrac{1}{2})(A_n + 3A_p)^2 ,$$
$$\frac{d\sigma}{d\Omega}(\pi^-, \theta_{\text{peak}}, J) \simeq C_J (J_f + \tfrac{1}{2})(3A_n + A_p)^2 , \qquad (3)$$

and Table I contains the numerical values of $C_J$ and the forms of transition density for neutrons and protons in terms of the matrix elements defined in Eq. (2).

In Table II we list the relevant transition density matrix elements for the low-lying states of $^{13}$C, together with the numerical values of estimated peak cross sections resulting from Eq. (3). Of course except for $J_f = \frac{9}{2}$ and $\frac{1}{2}$, two $J$ values contribute incoherently to the total cross section,

TABLE I. Parameters and form of transition density matrix elements used in the peak cross section estimates of Eq. (3) for 162 MeV pions on $^{13}$C.

| $J$ | $\theta_{\text{peak}}$ | $C_J$ ($\mu$b) | $A$ |
|---|---|---|---|
| 4 | 65° | 5.5 | $A_{4(31)d}$ |
| 3 | 45° | 19 | $A_{3(30)d}$ |
| 2 | 35° | 14 | $A_{2(11)d} + 0.55A_{2(11)s}$ |
| 1 | 20° | 300 | $A_{1(10)d} + 0.56A_{1(10)s}$ |

TABLE II. Transition density amplitudes $A_{J(LS)l}$ of neutrons and protons for the low lying states of $^{13}$C. The peak cross sections resulting from Eq. (3) are given in $\mu$b for each state. The asterisk indicates the second state of a given $J_f$.

| | | $J(LS)l$ | | | | | |
|---|---|---|---|---|---|---|---|
| $J_f$ | $t_3$ | 4(31)$d$ | 3(30)$d$ | 2(11)$d$ | 2(11)$s$ | 1(10)$d$ | 1(10)$s$ |
| $\frac{1}{2}$ | $n$ | | | | | −0.186 | 0.597 |
| | $p$ | | | | | −0.069 | 0.072 |
| | $\sigma^-$ | | | | | 52 | |
| | $\sigma^+$ | | | | | 1.2 | |
| $\frac{3}{2}$ | $n$ | | | 0.043 | −0.147 | −0.158 | 0.464 |
| | $p$ | | | −0.002 | −0.001 | −0.024 | 0.010 |
| | $\sigma^-$ | | | 0.4 | | 49 | |
| | $\sigma^+$ | | | 0.1 | | 1.4 | |
| $\frac{3}{2}$* | $n$ | | | 0.064 | −0.058 | −0.038 | 0.175 |
| | $p$ | | | 0.002 | −0.022 | −0.022 | −0.016 |
| | $\sigma^-$ | | | 0.2 | | 13 | |
| | $\sigma^+$ | | | 0.0 | | 0.7 | |
| $\frac{5}{2}$ | $n$ | | −0.485 | 0.306 | −0.090 | | |
| | $p$ | | −0.101 | 0.007 | 0.000 | | |
| | $\sigma^-$ | | 136 | 25 | | | |
| | $\sigma^+$ | | 35 | 3.3 | | | |
| $\frac{5}{2}$* | $n$ | | 0.071 | −0.187 | 0.554 | | |
| | $p$ | | −0.041 | 0.005 | −0.022 | | |
| | $\sigma^-$ | | 1.7 | 5.0 | | | |
| | $\sigma^+$ | | 0.2 | 0.4 | | | |
| $\frac{7}{2}$ | $n$ | 0.194 | −0.308 | | | | |
| | $p$ | −0.039 | −0.068 | | | | |
| | $\sigma^-$ | 6.5 | 74 | | | | |
| | $\sigma^+$ | 0.1 | 20 | | | | |
| $\frac{9}{2}$ | $n$ | 0.635 | | | | | |
| | $p$ | 0.001 | | | | | |
| | $\sigma^-$ | 100 | | | | | |
| | $\sigma^+$ | 11 | | | | | |

but from the shapes in Figs. 1–5 adjustment can be made to find the total at a given angle. By comparing the peak cross sections of Table II with the DWIA calculations for these states in Figs. 7–12, we see that the approximate values are good to 15% and usually much better for all cases where the magnitude is greater than 20 $\mu$b. For example the formulas give 74 $\mu$b for $\pi^-$ scattering to the $\frac{7}{2}^+$ state compared to the DWIA value of 75 $\mu$b, and 20 compared to 22 for $\pi^+$ scattering. Even the weak $J=2$ cross sections to $\frac{5}{2}^{+}$* are given to 20%. The very weak cross sections for $\pi^+$ scattering to $\frac{1}{2}^+$, $\frac{3}{2}^+$, and $\frac{3}{2}^{+}$* are not well represented, but Eq. (3) gives small values.

This approximation procedure thus offers a way to survey the many states at higher excitation for prominent transitions without doing extensive DWIA calculations.

### D. Survey of states at higher excitation energies

There are over 80 positive parity states in the range of 10 to 23 MeV of excitation energy within our $1\hbar\omega$ shell model space. Enlarging the space to include $3\hbar\omega$ excitation will produce some energy shifts and redistribution of transition strength. Nevertheless, our calculation should give a reasonable idea of the general location of strong transitions. An important feature of the amplitudes of Table I is that for $J=1$ and 2 the relative sign and magnitude of the $d$ and $s$ contributions are very similar to what one gets in calculating $E1$ and $M2$ transitions. The $J=3$ and 4 amplitudes are also clearly related to $E3$ and $M4$ transitions, so in order to see whether there is correlation between $(\pi,\pi')$ strength and calculated strength for inelastic electron scattering we include quantities relevant to $(e,e')$ in our survey. There are current experiments[6] on $^{13}$C with electrons of 200 MeV incident energy scattered by 180°, an arrangement which favors magnetic transitions. Our $M2$ and $M4$ cross sections are calculated for such conditions.

In Fig. 13 we give the peak cross sections at 65° for $\pi^-$ and $\pi^+$ scattering calculated from Eq. (3) for $J=4$ excitation of states with $J_f=\frac{9}{2}$ and $\frac{7}{2}$ in the range of 9.5 to 23 MeV. At the top of Fig. 13 are simple Born approximation values for the $M4$ cross section at 180°:

$$\left.\frac{d\sigma(M4)}{d\Omega}\right|_{180^\circ} = 95\times10^{-34}\ \mathrm{cm}^2\left(\frac{q}{5}\right)^8 \times \exp(-q^2/2\beta)B_{M4}(q=0), \qquad (4)$$

where the momentum transfer is $q(\mathrm{fm}^{-1})=(400-E^*)/\hbar c$ and we use the oscillator parameter $(2\beta)^{-1}=1.41\ \mathrm{fm}^2$. The $q$-dependent factor in Eq. (4) varies by only 10% for $10\leq E^*\leq 23$ MeV, so the relative cross sections are determined primarily by $B_{M4}(q=0)$. The general features of $J=4$ pion excitation in Fig. 13 show no cross section about 40 $\mu$b except the previously discussed $\frac{9}{2}$ state at 9.5 MeV. Between 15 and 17 MeV, $\pi^+$ excitation is calculated to be stronger than $\pi^-$ excitation, while from 19 to 23 MeV, $\pi^\pm$ strength is of comparable magnitude with many states contributing. In electron scattering fewer states contribute and only 4 are calculated to be

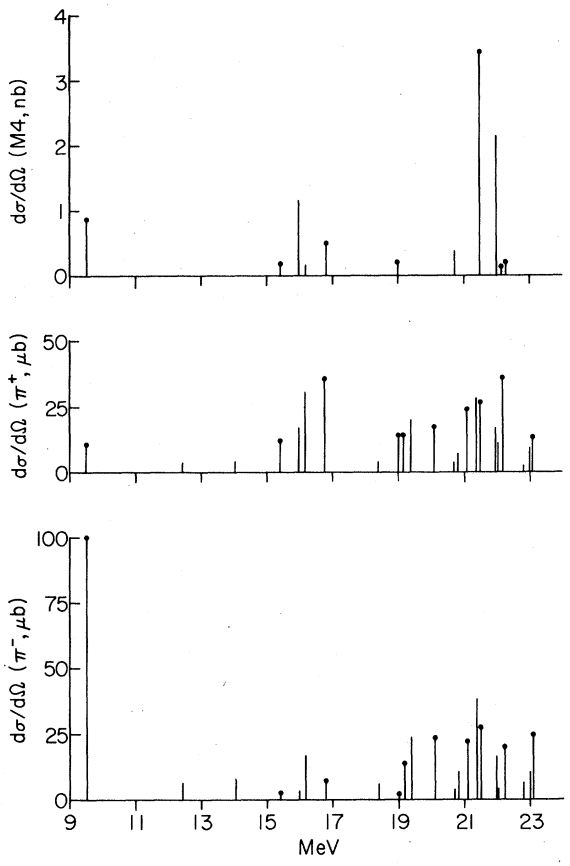


FIG. 13. Cross sections at 65° for $J(LS)=4(31)$ scattering of 162 MeV pions on $^{13}C$ given by Eq. (3). The $\pi^-$ values are at the bottom and $\pi^+$ values in the center and states have $J_f=\frac{7}{2}$ or $J_f=\frac{9}{2}$ (rounded top). At the top are cross sections for $(e,e')$ at 180° with 200 MeV incident electrons given by Eq. (4).

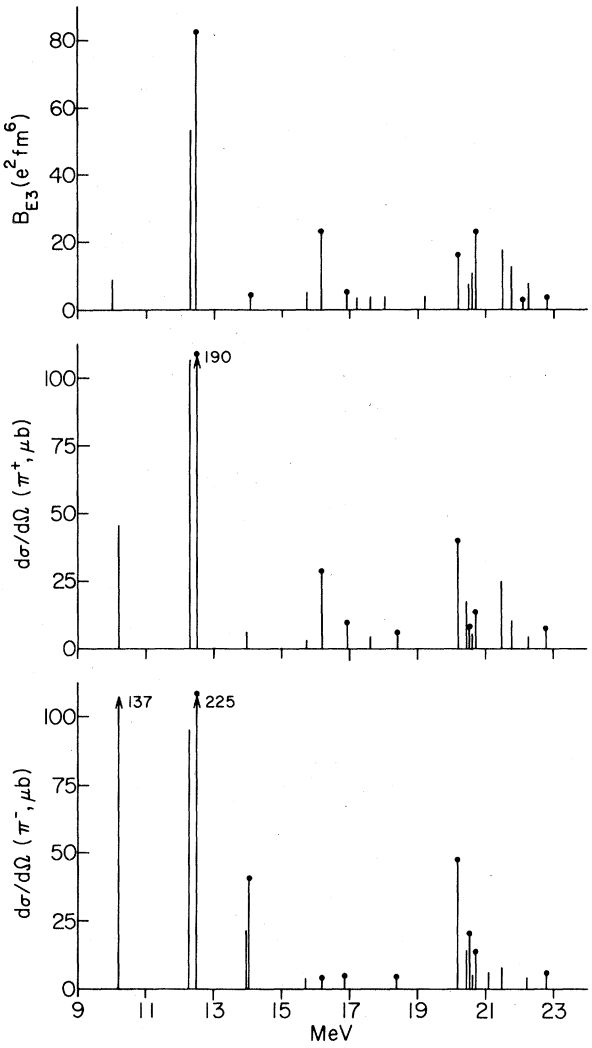


FIG. 14. Cross sections at 45° for $J(LS)=3(30)$ scattering of 162 MeV pions on $^{13}C$ given by Eq. (3). The $\pi^-$ values are at the bottom and $\pi^+$ values in the center and states have $J_f=\frac{5}{2}$ or $J_f=\frac{7}{2}$ (rounded top). At the top are $B_{E3}(q=0)$ values to indicate relative cross sections in electron scattering.

prominent, namely $\frac{9}{2}$ states at 9.5 and 21.5 MeV and $\frac{7}{2}$ states at 16 and 22 MeV. On the question of $(\pi,\pi')$ correlation with $(e,e')$, consider the 4 states between 15 and 17 MeV which appear in both reactions. The $J_f=\frac{7}{2}$ state at 16 MeV is dominant in $(e,e')$ but makes only a modest contribution in $(\pi,\pi')$. On the other hand, the $J_f=\frac{7}{2}$ state at 16.2 MeV is weak in $(e,e')$ but prominent in $(\pi^+,\pi^{+\prime})$ where it incidently also has strength in $J=3$ excitation. Similarly at 21.5 MeV, the $J_f=\frac{9}{2}$ state (which has $T=\frac{3}{2}$) is strong in $(e,e')$ and also in $(\pi,\pi')$, but a nearby $J_f=\frac{7}{2}$ state (which has $T=\frac{1}{2}$) is absent in $(e,e')$ but has strength comparable to the $\frac{9}{2}$ state for $(\pi,\pi')$. Thus there is some correlation between the reactions, but the prominent peaks are not necessarily due to the same states in both reactions.

In Fig. 14 we give the peak cross sections at 45° for $\pi^-$ and $\pi^+$ scattering calculated from Eq. (3) for $J(LS)=3(30)$ excitation of $J_f=\frac{7}{2}$ and $\frac{5}{2}$ states. Since the relative cross sections for $(e,e')$ excitation of these states at forward angles are not strongly $q$ dependent, we give $B_{E3}(q=0)$ values at the top of Fig. 14. There are three strong transitions in Fig. 14: one a $J_f=\frac{5}{2}$ state at 10.2 MeV with $\pi^-$ excitation favored over $\pi^+$ by a factor of 2.7 and not prominent in $(e,e')$; the other two a pair of states near 12.4 MeV which are prominent in all three reactions and mainly isoscalar. The lower state has $J_f=\frac{5}{2}$ and the upper $J_f=\frac{7}{2}$ has the largest calculated cross sections (about 200 $\mu$b) for both $\pi^+$ and $\pi^-$ excitation of the positive parity states below 23 MeV. Aside from these states there is some strength for $\pi^+$ and electron excitation of the $J_f=\frac{7}{2}$ state at 16.2

MeV, which was discussed above for $J=4$ excitation, and little else is seen between 15 and 20 MeV. Between 20 and 21 MeV there is some more calculated strength for $J=3$ excitation, particularly for a $J_f=\frac{7}{2}$ state just above 20 MeV.

It is known that collective states, such as the $J=3^-$ state at 9.64 MeV in $^{12}$C, have $B_{E3}$ values that are enhanced over values obtained from a calculation in $1\hbar\omega$ space, and that a similar enhancement is required[7] for inelastic pion scattering. The question arises whether the $J_f=\frac{5}{2}$ and $\frac{7}{2}$ states of $^{13}$C near 12 MeV have the simple structure of a $p_{1/2}$ neutron coupled to the $3^-$ state of $^{12}$C and thus also need enhancement. Expansion of our wave functions in terms of $p$ nucleons coupled to negative parity states of $^{12}$C shows that such a simple picture is not valid, there being many terms of magnitude comparable to that of $p_{1/2}\times 3^-$. Since the $^{13}$C ground state also has many terms in such a parentage expansion this procedure casts no light on the nature of these $E3$ transitions and does not suggest that they should be enhanced beyond our calculated values.

In Fig. 15 we give the peak cross sections at 35° for $\pi^-$ and $\pi^+$ scattering calculated from Eq. (3) for $J(LS)=2(11)$ excitation of $J_f=\frac{5}{2}$ and $\frac{3}{2}$ states. At the top are Born approximation values for the $M2$ cross section at 180° for 200 MeV incident electrons given by

$$\left.\frac{d\sigma(M2)}{d\Omega}\right|_{180^\circ} = 722\times10^{-34}\ \mathrm{cm}^2\left(\frac{q}{5}\right)^4 B_{M2}(q)\,. \qquad (5)$$

However, for this lower multipole several of the single particle $M2$ matrix elements are near minimum values for $q=2$ fm$^{-1}$ and others have changed sign from their $q=0$ values, so the $B_{M2}(q=2)$ values are generally much smaller than the $B_{M2}(q=0)$ values and bear little resemblance to them. While we have included $[Y^3\times\sigma]$ contributions to these $M2$ cross sections, the use of oscillator wave functions beyond the first minimum in $q$ is suspect, so our values for the $(e,e')$ cross sections are crude estimates at best. They do suggest generally weak cross sections, since even the two largest values at about 19 MeV are only 7 to $8\times10^{-34}$ cm$^2$. The $J=2$ pion cross sections show only a few prominent peaks, one being the $J_f=\frac{5}{2}$ state at 10.2 MeV which has appreciable $\pi^-$ cross section to add to the strength it had for $J=3$ excitation. The strongest cross section occurs for a $J_f=\frac{5}{2}$ state at 14 MeV with about 120 $\mu$b for $\pi^-$ excitation and only 10 $\mu$b for $\pi^+$ excitation. There are also two states around 17.5 MeV which have about twice the cross section for $\pi^+$ excitation as for $\pi^-$ excitation. Otherwise little strength is predicted and there is little correlation with $(e,e')$ strength.

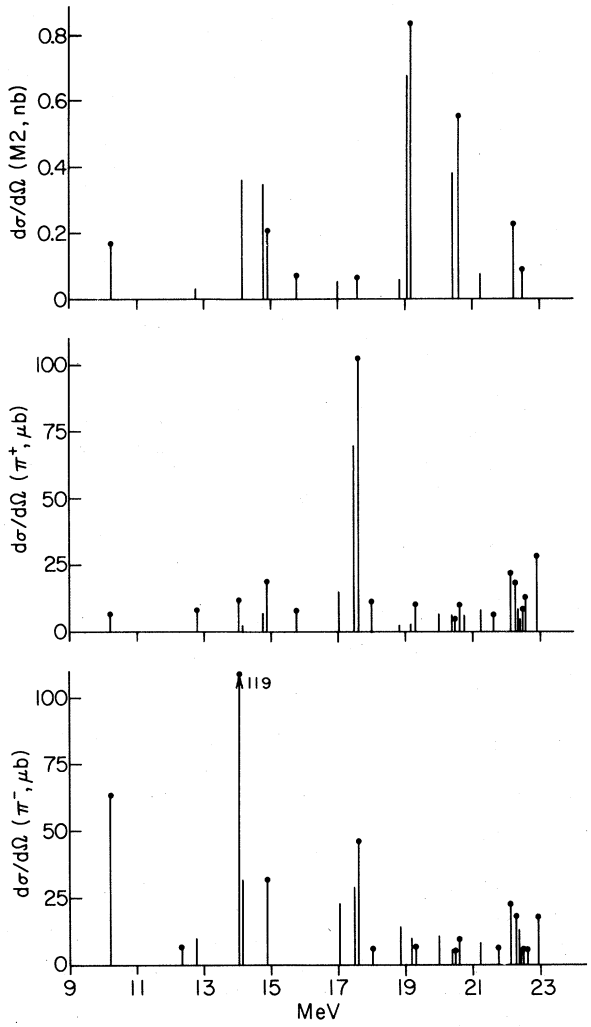


FIG. 15. Cross sections at 35° for $J(LS)=2(11)$ scattering of 162 MeV pions on $^{13}$C given by Eq. (3). The $\pi^-$ values are at the bottom and $\pi^+$ values in the center and states have $J_f=\frac{3}{2}$ or $J_f=\frac{5}{2}$ (rounded top). At the top are cross sections for $(e,e')$ at 180° with 200 MeV incident electrons given by Eq. (5).

In Fig. 16 we give peak cross sections at 20° for $\pi^-$ and $\pi^+$ scattering calculated from Eq. (3) for $J(LS)=1(10)$ excitation of $J_f=\frac{3}{2}$ and $\frac{1}{2}$ states. At the top we list values for $B_{E1}(q=0)$ which are adequate for $(e,e')$ at low momentum transfer; at higher $q$ there will be large changes in relative magnitudes due to oscillation of the form factor as was the case for $M2$ excitation, but $E1$ excitation can be measured at relatively low $q$. There are 4 prominent states excited in pion scattering with cross sections from 75 to 120 $\mu$b. The lowest in energy is a $J_f=\frac{3}{2}$ state at 12.8 MeV with 75 $\mu$b cross section in $\pi^+$, negligible $\pi^-$ cross section, and weak $B_{E1}$ value. The other three states, at 15.3, 18.8, and 21.2 MeV, all have cross sec-

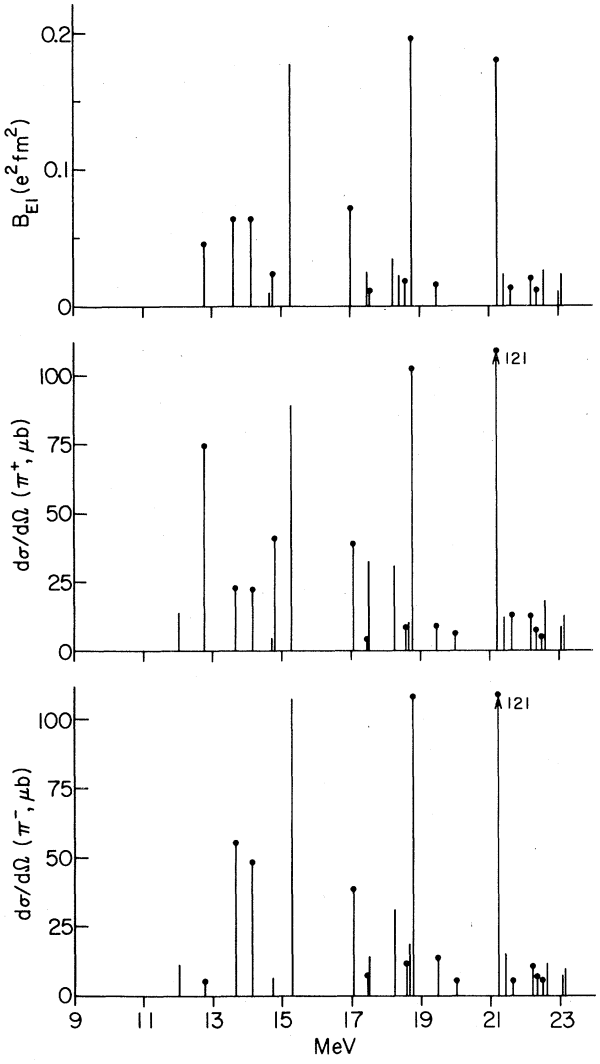


FIG. 16. Cross sections at 20° for $J(LS)=1(10)$ scattering of 162 MeV pions on $^{13}C$ given by Eq. (3). The $\pi^-$ values are at the bottom and $\pi^+$ values in the center and states have $J_f=\frac{1}{2}$ or $J_f=\frac{3}{2}$ (rounded top). At the top are $B_{E1}(q=0)$ values to indicate relative cross sections in electron scattering.

tions of about 100 $\mu$b for both $\pi^+$ and $\pi^-$ excitation, and also have the largest $B_{E1}$ values in this energy region. There are also some strong transitions calculated to be in the region of the giant $E1$ resonance, the strongest being a $J_f=\frac{3}{2}$, $T=\frac{3}{2}$ state at about 25 MeV with calculated $\pi^\pm$ cross sections of 300 $\mu$b. All of these states would only be strong near 20° since as shown in Figs. 4 and 5 they should be weaker by at least an order of magnitude for angles above 40°.

## IV. DISCUSSION AND SUMMARY

The cross sections for exciting states of non-normal parity in $^{13}C$ by $(\pi,\pi')$ show about 10 transitions with strength of 100 to 200 $\mu$b, and many in the range of 50 to 100 $\mu$b. Such magnitudes are comparable to those for exciting normal parity states except for the few collective $L=2$ $S=0$ states which have cross sections of about 1 mb and include enhancement factors[1] for the calculated values. Furthermore, many of the strong non-normal parity transitions occur for higher excitation energy where normal parity transitions are calculated to be weak.

The strong transitions are often dominated by a single $J(LS)$ amplitude, and we have shown that these have distinctive shapes and that the results of DWIA calculations for peak cross sections are well approximated by simple formulas. The constants $C_J$ in Table I probably change slowly with mass number [in the normal parity transitions we found[1] that the $(LS)=(20)$ constant varied as $A^{-1}$] so that Eq. (3) can be used to estimate $(\pi,\pi')$ cross sections for nearby nuclei like $^{12}C$ and $^{14}N$ given the nuclear structure input and a factor $(J_i+\frac{1}{2})^{-1}$.

In $^{13}C$ we find interesting behavior of the ratio of cross sections in comparing $\pi^-$ with $\pi^+$ scattering. For the low lying states, $\pi^-$ is favored and this results from the dominant nature of these states as neutrons coupled to $T=0$ states of $^{12}C$. In the region of 15 to 19 MeV excitation there is a preponderance of strong transitions favoring $\pi^+$ over $\pi^-$ scattering [except for $J(LS)=1(10)$]. This behavior is attributable to the nuclear structure feature that these states have strong parentage to the lowest $T=1$ states of the $A=12$ system, a property favoring $\pi^+$ transitions. Above 19 MeV $\pi^\pm$ excitation is roughly of equal strength. These are general features, and there are individual states which do not obey the general trend. The comparison of data with our calculations will be presented in a separate publication,[4] and it will be interesting to see to what extent our results for strong transitions are valid. For the region of Figs. 13–16 our results can only be a general indication of strength localization since we have neglected the effects of 3p-3h excitations and the continuum. As far as correlation between $(\pi,\pi')$ and $(e,e')$ we find good correlation between prominent states for electric transitions, $E1$ and $E3$, but not much for $M2$ and $M4$.

For weak states there are other effects not included in our DWIA which may be important. One is the contribution from $L=2$ and $L=0$ amplitudes of the transition density. In the nuclear structure calculation these are often as large as the $L=3$ and $L=1$ amplitudes, but they are excluded from the DWIA by the factorization approximation.[8] These even $L$ amplitudes should be included if a more careful treatment is desired.

Another factor for weak transitions is the coupling to stronger channels. However, such treatments present an order of magnitude of greater calculation diffuclty. For the moment we want to see how well this simplest approach succeeds in representing observations.

ACKNOWLEDGMENTS

We wish to thank the authors of Ref. 3 for discussion and permission to present their data in Fig. 12. This work was performed under the auspices of the U. S. Dept. of Energy.

[1]T.-S. H. Lee and D. Kurath, Phys. Rev. C 21, 293 (1980).
[2]D. J. Millener and D. Kurath, Nucl. Phys. A255, 315 (1975).
[3]D. Dehnhard, S. J. Tripp, M. A. Franey, G. S. Kyle, C. L. Morris, R. L. Boudrie, J. Piffaretti, and H. A. Thiessen, Phys. Rev. Lett. 43, 1091 (1979).
[4]S. J. Tripp *et al.* (unpublished).
[5]E. Schwarz, J.-P. Egger, F. Goetz, P. Gretillat, C. Lunke, C. Perrin, B. M. Preedom, and R. E. Mischke, Phys. Rev. Lett. 43, 1578 (1979).
[6]R. Hicks *et al.*, LASL Report No. LA-8303-C, 1980, p. 292.
[7]T.-S. H. Lee and F. Tabakin, Nucl. Phys. A226, 253 (1974).
[8]The factorization approximation is recently discussed in A. W. Thomas and R. H. Landau, Phys. Rep. C58, 121 (1980).